HIGH SPEED PERMANENT MAGNET BRUSHLESS MOTORS FOR SPINDLES AND COMPRESSORS.

JAMES R. HENDERSHOT JR
P.O. BOX 78
HILLSBORO, OHIO 45133
(513)-393-3810

1. INTRODUCTION

The advantages of High Speed Electric motors have been known for a very long time. In recent years the interest in high speed machines has intensified for several reasons. However the main reason is due to the availability of high power switching semiconductors now being utilized for invertors with high speed controllers using DSP's or other microprocessors.

The most common electric machine currently in use for high speed high power operation is the polyphase A.C. induction motor. These specially designed machines are available from only three companies in the USA with one of them clearly the leading supplier. A very good supplier also exists in Switzerland. There are a couple in Germany and a few other scattered around Europe. Japan is reported to have a couple of suppliers as well.

These high speed induction motors are principally used for machine tool spindles such as drilling, grinding and milling. They are driven by high frequency invertors with only two suppliers in the USA with capabilities to 3 KHZ output frequency, (equivalent to 180 KRPM for a 2 pole motor or 90 KRPM for a 4 pole motor. Speed is a function of frequency (f) and the number of poles.

$$SPEED = \frac{f \times 120}{poles} \quad \text{RPM} \qquad (1)$$

The ability of a given motor structure to remain functional at such high speeds depends upon its diameter after the shaft / bearing dynamics have been designed for operational integrity. The rotor diameter of an induction motor (along with its length) determines the output torque which times speed equals the motors output power. Therefore the present high speed machines exhibit a direct relationship between their speed and output power due to the structural limitations of the induction motor rotor. Figure 1 shows a typical cross section of the rotor of an induction motor.

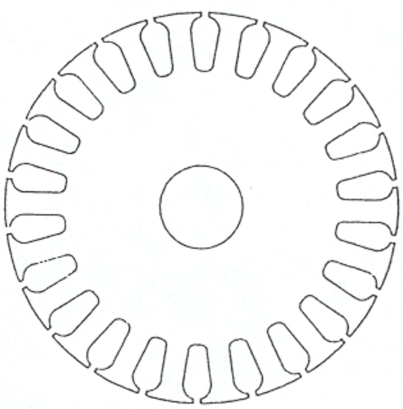

FIG. 1 ROTOR , A.C. INDUCTION

The slots at the surface of the rotor laminations are filled with either aluminum or copper bars attached to end rings of the same corresponding material. The laminations are soft magnetic iron with relatively low mechanical strength.

When these rotors spin at high speeds, there exists a max stress limit for each rotor design (diameter & length). Otherwise the lamination yields at the slot openings and copper and aluminum bars in the slots are forced radially causing immediate out of balance and final rubbing on the stator I.D. Several techniques or design modifications are used to control this problem.

The iron losses in the induction motor rotor and the I^2R losses in the conductors (aluminum or copper commonly called the "squirrel cage") cause considerable rotor heating. The cooling of the rotors in these high speed machines is a very difficult problem to deal with. Some method of cooling is usually employed to get rid of the rotor heating in the rotor.

Many of the current high speed motor applications require much higher output powers or torques than previous high speed applications. A partial listing of these current applications is listed or reference.

MILLING MACHINE SPINDLES
GRINDER SPINDLES
CENTRIFUGAL AIR COMPRESSORS
CENTRIFUGAL REFRIGERANT COMPRESSORS
GAS TURBINE STARTER / GENERATORS
FLYWHEEL MOTOR / GENERATORS
CENTRIFUGAL LUBE AND FUEL PUMPS
OIL WELL CENTRIFUGES
INDUSTRIAL & MEDICAL CENTRIFUGES

2. FEASIBLE HIGH SPEED MOTOR CHOICES FOR MEDIUM TO HIGH POWER

There are basically three electric motor choices for high speed applications. The induction motor is the most widely used motor. It's problems or limitations have been discussed. It should be the motor of choice if possible due to its availability and cost. Most leading manufactures of high performance, high speed induction motors agree that the current rotor materials and rotor retainment systems limit this type of a machine to less than 50,000 RPM at 50 KW output (known as a 50 / 50). If either the speed or output power is increased beyond 50 / 50 the induction motor rotor will not survive according to the induction motor experts.

Another choice is the brushless D.C. motor without permanent magnets known as the Switched Reluctance machine. The principle advantage of the SR brushless motor is its simple and robust rotor. (Shown on figure 2)

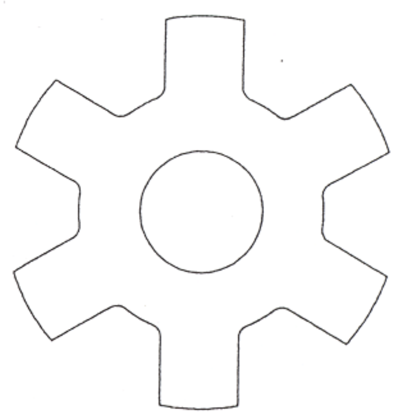

FIG. 2 SR ROTOR

The construction of this rotor consists of a stack of gear shaped stampings of motor lamination material fastened to the motor shaft. The rotor contains no windings, conductors, coils or a squirrel cage. Therefore its centrifugal integrity is determined by the yield strength of the rotor lamination material. These types of machines have been used at 60,000 RPM on large gas turbine starter generators (up to 250 KW) as well as some high speed centrifugal jet fuel pumps. Smaller SR units have been designed for 100 KRPM.

The SR machine has no I^2R losses because it contains no electric current carrying conductors as previously stated. However the rotor laminations are subjected to a $d\Phi/dt$ which causes both eddy current and hystersis heating losses. This magnetic flux is induced from the mmf from the eletro-magnetic stator. It cannot be avoided or circumvented by design as is somewhat possible with the induction motor. Therefore the SR machine also requires a method of cooling the rotor (although not as severe a problem as with the induction motor rotor). For high speed power output, the SR has more potential than the AC induction motor and somewhat higher power density and slightly higher efficiency. The SR brushless motor probably would cost more than the induction over the short term because the SR is not nearly as widely available as the AC induction motor.

The third type of electric machine useful for high speed, high power operation is the permanent magnet brushless motor known as PM brushless. Although there are many different PM brushless rotor configurations possible, Figure 3 illustrates one of the most practical for high speed operation.

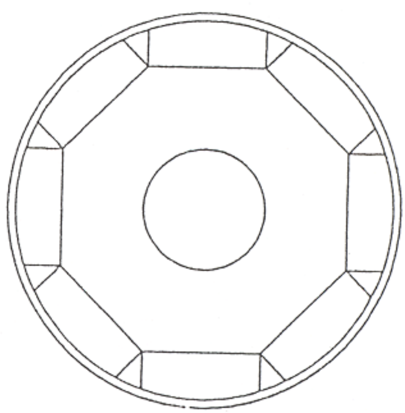

FIG. 3 PM BRUSHLESS ROTOR

The magnets are always of the rare earth type which are attached to either a laminated stack for the rotor back iron/ core or a solid shaft made from alloy steel. The magnets are then precisely secured with a carefully designed magnet retainment system to assure rotor integrity at all operating speeds and temperatures. Unless the rotor is properly designed, excessive heating can develop in any portion of the rotor at high speeds. Otherwise the PM brushless rotor is the "coolest of the three".

3. MOTOR SELECTION FOR HIGH SPEED MULTI-AXIS MACHINE TOOL SPINDLE

The first consideration before a motor is selected made has to be the basic requirements of each application. Therefore the first application discussed here is the high powered milling machine tool spindle which must put out a constant HP over a very wide speed range. For example there are two very common requirements. The 40 HP spindle must produce increasing torque as the

RPM decreases from 20,000 RPM down to 2500 RPM for a constant HP range over a speed range of 8:1 another similar application is a 75 constant HP spindle from12,500 RPM to 2500 RPM or a 5:1 increase in output torque as RPM decreases. Figure 4 shows a typical cross section of a high speed PM brushless motor fitted into a milling machine spindle.

The motor-rotor and stator are assembled into the spindle between the bearings as shown. The bearings can be ceramic ball, foil, air bearings, fluid bearings or active magnetic bearings. Fluid bearings are shown in Figure 4. The stator is always water cooled and fitted with thermal couples, one in each phase for temperature monitoring. The most important issues or requirements of these types of constant HP spindles are listed as follows:

- Wide constant power range
- Small physical size (high power density)
- Continuous operation at both low and high RPM
- Thermally stable
- High axial and radial stiffness
- Long life without maintenance

These new types of multi-axis machine tools provide the optimum of flexible manufacturing using high acceleration linear PM brushless motors, fast tool changing, and CNC computer controls. All three motors, AC induction, SR brushless and PM brushless can be easily packaged between the front and rear spindle bearings for these HP's and speeds no matter which bearings are used. Similar variable speed invertors can be built using either IGBT or MOSFET power transistors. However due to the mechanical requirements of the spindle and thermal considerations all three motor choices are not equivalent and useful. For example, these spindles must be extremely rugged and able to withstand extremely high radial and axial stiffness during the cutting operation. This is an absolute requirement in order to achieve surface finish and accuracy. This requirement necessitates the use of very large shafts and bearings. In addition to the section modules required from a large shaft, a hole must be used down the center of the spindle shaft. These CNC multi-axis machines use automatic tool changers. A thru-shaft draw bar is used to secure the tool in its holder on the spindle nose. The large shaft diameter is a natural friend to the PM brushless motor designed to be fitted between the front and rear bearings. On the other hand the large diameter shaft is a significant problem for the AC induction motor or SR brushless motor. Both the AC and SR motors must be constructed with laminated rotors with a sufficient yoke thickness to carry the flux from pole to pole. This section of the yoke must be laminated in both of these motors because the flux changes during rotation causing heating. The AC induction motor requires space for conductors to form the squirrel cage and the SR brushless requires radial salient poles beyond the yoke. In both cases the rotor is much larger than the PM brushless rotor. Since the permanent magnet yoke or back iron in the PM brushless motors need not to be laminated, the rotor is only slightly larger than the spindle shaft. The alloy steel shaft of the spindle is used for the back iron. The magnets are secured directly to the shaft of the spindle with a retention system. This type of PM brushless motor results in the smallest motor package which is possible to fit between the bearings of these large spindles. The two reasons for this both result from the use of high energy permanent magnets for the rotor flux production. The magnets are relatively thin and produce a very high magnetic flux and they are attached directly onto the spindle shaft or tube without a lamination structure for back iron. The other

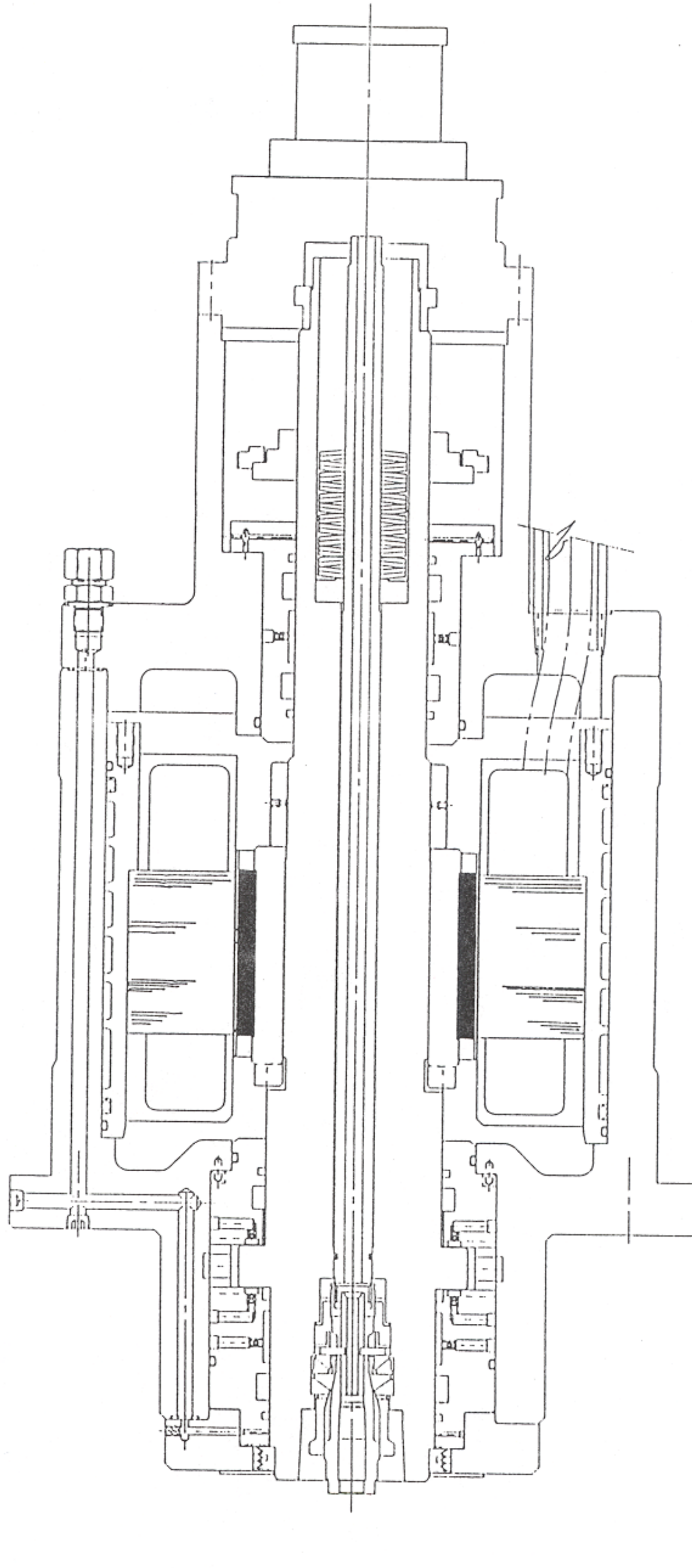

FIG. 4 50 HP, 20 KRPM BRUSHLESS SPINDLE

Its corrosion tendency makes NEO very difficult to use on a shaft or tube which is ground after placing magnets. There seems to be no way to be sure corrosion has not begun before the retainment sleeve is wrapped and cured. On lower speed motors a pre-machined sleeve could be shrink fitted over ground NEO magnets. However for this application the resistivity of the INCONEL sleeve is not high enough to prevent eddy currents in the ring and over heating of the rotor.

These spindles are so expensive that the risks associated with using NEO far outweighs the cost advantage of NEO. We have found that Samarium costs 1.5 times NEO for best materials of each type. The operation temperature actually allows for the same gap flux for both. The NEO has no advantage and only problems to deal with. Note: These motors with constant HP over a wide speed range experience very high demagnetizing currents at the trailing pole edges at low speeds.

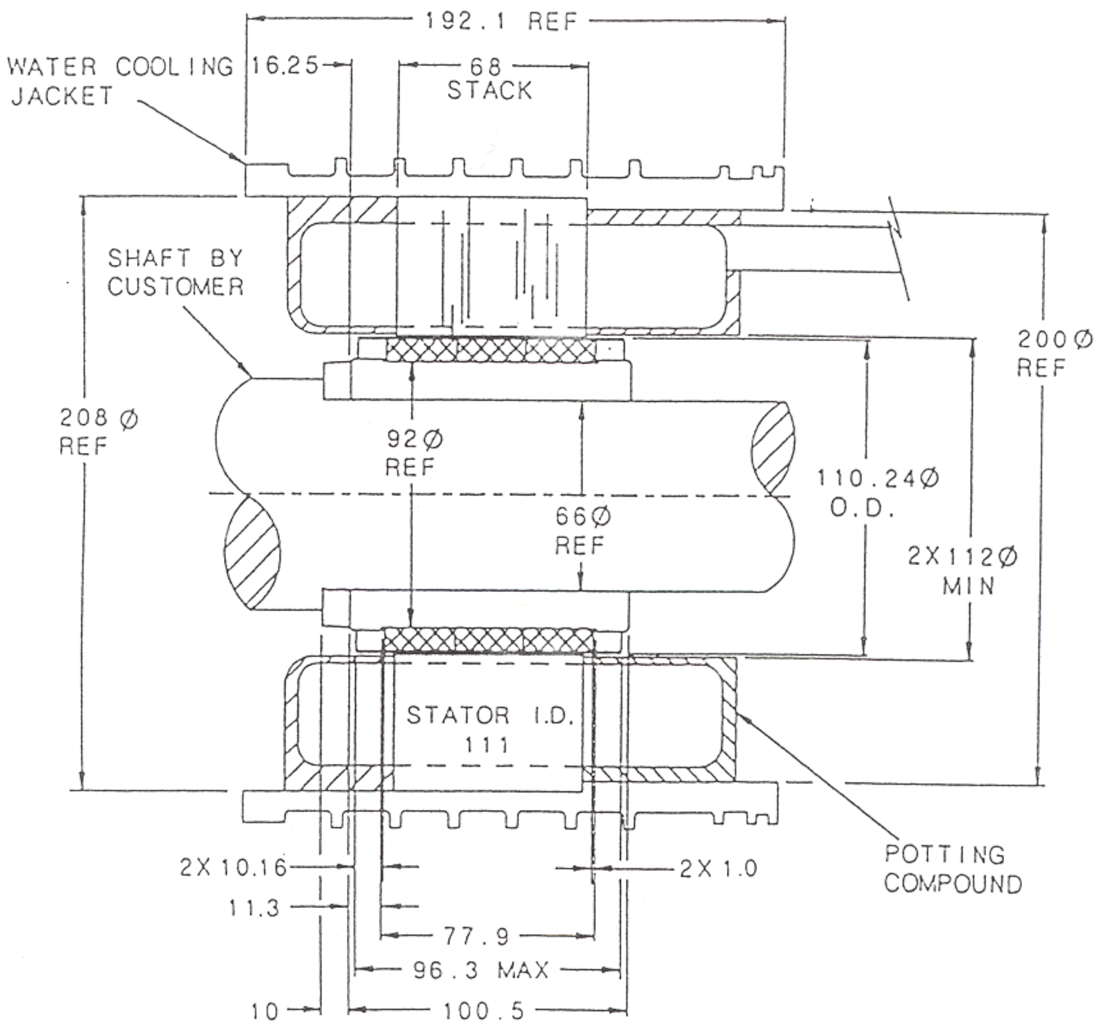

FIG. 5 50 HP, 20 KRPM PM BRUSHLESS DC MOTOR

important feature which is important in these machine tool spindles if the relatively low heating of the PM rotor (if properly designed).

4. 50 CONSTANT HP PM BRUSHESS SPINDLE MOTOR

A few years ago a parametric design study was done to compare the three motor technologies. The customer supplied the data for the AC induction motor which was a four pole machine which accounts for some of its size and weight. Both SR and PM brushless motors were optimized for comparison. The mechanical data is summarized in table A for the (3) 75 HP water cooled motors.

The final design changed considerably from the original study but the results were clear as to which motor type to select based upon size and weight with a 4.75" dia shaft as a given.

The actual 75 HP PM motors made for this application are confidential at the date of this paper due to the various features of the spindle including the shaft material, bearings and actual motor design. The actual stator O.D. was somewhat smaller and it was slightly longer than the original design. It produced constant HP over the speed range of 2500 to 12,000 RPM and in fact the peak HP was over 150 at 10,000 RPM.

An actual example of a 50 HP spindle motor spindle motor using 6 poles and 8.188" O.D. stator is given for an example of these types of machine tool spindle motors. The constant HP range for this spindle was 3500 to 20,000 RPM. The rotor bearings were so small that the magnets were attached to a soft iron tube and then wrapped with prestressed composite yarn of carbon fiber and bonded with a high temperature epoxy (180°). The magnet grade was 27 MGO Samarium Cobalt. Neo was not selected due to its temperature coefficient with B and in particular H.

TABLE 1

	AC INDUCTION	SR BRUSHLESS	PB RUSHLESS
STATOR O.D.	14.76"	12.50"	9.448"
STATOR I.D.	8.47"	8.10"	5.906"
STACK LG.	11.42"	7.00"	5.000"
ROTOR O.D.	8.30"	8.00"	5.786"
ROTOR I.D.	4.75"	4.75"	4.75"
ROTOR LG.	11.42"	7.00"	5.00"
AIR GAP	.040"	.035"	.025"
COPPER WT	?	13 lbs.	7 lbs.
IRON WT	?	147 lbs.	62.5 lbs.
MAG. WT	-0-	-0-	8.5 lbs.
TOT WT	350 lbs.	160 lbs.	78 lbs.
NUMBER POLES	4	6	8

Its corrosion tendency makes NEO very difficult to use on a shaft or tube which is ground after placing magnets. There seems to be no way to be sure corrosion has not begun before the retainment sleeve is wrapped and cured. On lower speed motors a pre-machined sleeve could be shrink fitted over ground NEO magnets. However for this application the resistivity of the INCONEL sleeve is not high enough to prevent eddy currents in the ring and over heating of the rotor.

These spindles are so expensive that the risks associated with using NEO far outweighs the cost advantage of NEO. We have found that Samarium costs 1.5 times NEO for best materials of each type. The operation temperature actually allows for the same gap flux for both. The NEO has no advantage and only problems to deal with. Note: These motors with constant HP over a wide speed range experience very high demagnetizing currents at the trailing pole edges at low speeds.

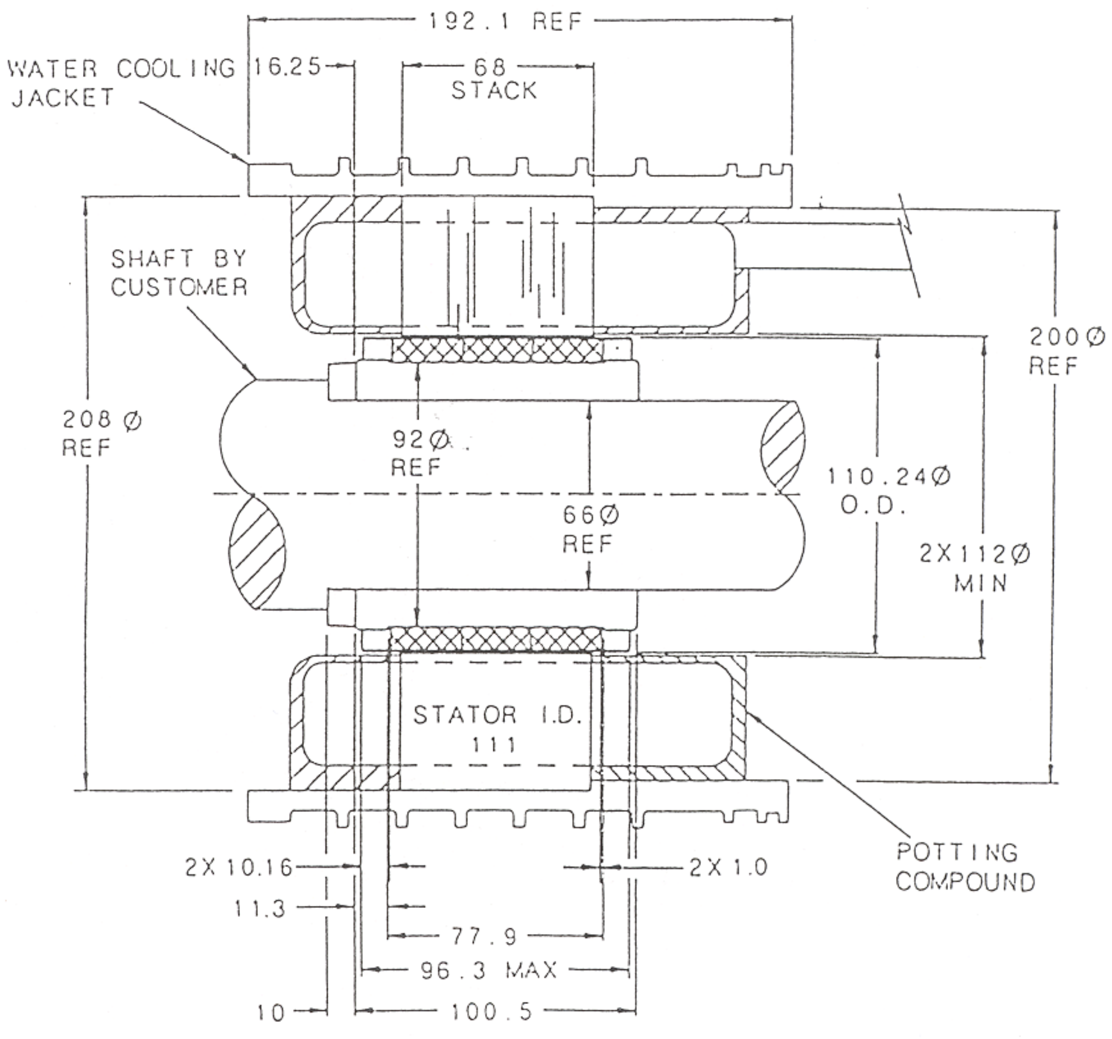

FIG. 5 50 HP, 20 KRPM PM BRUSHLESS DC MOTOR

Figure 5 shows the cross section of the 50 HP motor. The actual metric dimensions are given to illustrate the power density possible with these water cooled PM brushless machines. Figure 6 shows the cross section of the rotor stator which is a print out of the "cross section edit" from the design simulation software used for design (PC-BDC from the University of Glasgow by Dr. TJE Miller). The design simulation data for 3500 RPM is given in TABLE 2A and TABLE 2B. The winding is short pitched design to eliminate the 3rd harmonic otherwise present on a 6 pole 36 slot design. The winding arrangement is shown on Figure 7 with 6 turns per coil of 36 conductor in hand to minimize the skim affect and winding eddy currents. The coils of only a single phase is shown with the other two phases offset 4 slots from each other yielding 12 conductors per slot for a total of 432 (Z). The torque and performance is calculated dynamically at speed in time steps by integration forcing simi-wave currents into each phase. The putout power yielded 54.45 HP at 3500 RPM and 92.52% efficiency with 123.47 ARMS phase current.

Figure 8 shows the sinecurrent, back EMF & torque vs rotation angle. The air gap flux is plotted or Figure 9 showing both the open current flux distribution vs angle and a super imposed flux distribution with sine currents of 123.47 ARMS per phase. The flux at the leading edge increases and the flux at the trailing edge decreases but no permanent de-mag occurs using the 26 MGO Samarium magnets.

The output data for the performance of this design is shown on TABLE 3A and 3B for 20,000 RPM. The output power is 54.9 HP at 20,000 RPM at 94% efficiency with 57 ARMS phase current. With the same winding of 6 turns per coil the back EMF would be much greater than the DC rail voltage. Although phase advancing would have been a possibility, the inverter manufacturer did not wish to commit to the program using this method of achieving constant power over such a wide speed range. Therefore several other methods of reducing the back EMF were considered, a list of the possibilities are given all of which involve using relays or contactors to switch winding configurations.

Wye-delta	K_e ratio	1.732:1	6 leads
Series-parallel	K_e ratio	2:1	12 leads
Single-tapped	K_e ratio	2:1	6 leads

The single tapped winding choice was made which requires only 6 leads (#4 AWG) out of the motor and a single switch with (3) poles and double throw. The resulting winding was 6 turns per coil at the lower RPM's and 3 turns per coil at higher speed. It turns out that it is possible to switch at speed (without load).

The (3) turn high speed winding is shown on Figure 10. The current, back EMF and torque vs rotor angle is shown on Figure 11. The air gap flux distribution vs angle is shown on figure 12.

TABLE 2A

PC-BDC 4.35Ã: 25th Mar 1996 22:05 50ING3K.BD4
JR Hendershot Magna Physics Tridelta
PC-BDC Main Title
PC-BDC Sub-title

1 Dimensions:--

RadSH	33.000 mm	Rad1	54.000 mm	Gap	1.500 mm
LM	8.000 mm	BetaM	147.000 eDeg	POLES	6
Rad2	89.000 mm	Rad3	104.000 mm	SLOTS	36
Tw	5.500 mm	SltDpth	33.500 mm	SltOpen	3.000 mm
SltODpth	1.000 mm	SltOAng	45.000 mDeg	RNSQ	Round
SYoke	15.000 mm	RYoke	6.837 mm	Skew	0.670
Lstk	67.000 mm	Stf	0.970	MOH	4.000 mm

2 Magnet Data:--

Magnet	R26H	RotType	SurfPll	Pm0	0.264 uWb/A-t
Br	1.060 T	HcJ	10.179 kOe	MuRec	1.020
CBr	-0.030 %/DegC	CHcJ	-0.030 %/DegC	DMag	8400.000 kg/m3

3 Control Data:--

Drive	Sine	Vs	640.000 V	RPM	3500.000 rpm
ISP	175.000 A	gamma	0.000 deg	Sw_Ctl	ISP_HB
Vq	3.000 V	Rq	0.000 Ohms	Vd	1.200 V
ISP_Act	175.000 A	HBA_Act	16.000 %	ISLA_Act	2.000

4 Winding Data:--

WdgType	Custom	Connex	3-Ph Wye		
Offset	4	Coils/P	2.000	NSH	36
Tph	72.000	PPATHS	1	SPP	2.000
Layers	2.000	CSidesPh	24	Z	432.000
MLT	337.439 mm	LgthOEnd	137.571 mm	Ext	8.000 mm
EndFill	0.500	LaxPack	119.741 mm	TFRho	1.217
SFill	0.397	Gauge	24.000	WireSpec	AWGTable
SFillHBL	0.688	WireDia	0.511 mm	Liner	0.254 mm
SlotArea	222.658 mm^2	CondArea	7.370 mm^2	ASlotLL	203.826 mm^2
WdgTemp	75.000 DegC	Rph	0.068 Ohm/Ph	Rterm	0.136 Ohms
Lph	0.544 mH/Ph	Mph	-0.238 mH/Ph	Lterm	1.564 mH
Lg	0.300 mH/Ph	LSlot	0.176 mH/Ph	Lendt	0.068 mH/Ph
Mg	-0.150 mH/Ph	MSlot	-0.088 mH/Ph	fz	1.142
PCSlot	2.415	XLph	1.000	XET	1.000
Ax1	38.350 mDeg				
iA_Ang	-159.743 A	iB_Ang	143.114 A	iC_Ang	16.629 A
ks1	0.995	kp1	0.837	kd1	1.000
kw1	0.832	Xm0	2.925 Ohm/Ph	Xd	0.745 Ohm/Ph
Nse	76.294	Xsigma	0.268	Xq	0.742 Ohm/Ph
Cd	0.163	Cq	0.162	k1	0.000
k1ad	0.000	k1aq	0.000	kAlphad	0.000
NumPoly	1				

TABLE 2B

5 Magnetic Circuit Design:--

BrT	1.043	T	BgOC	0.797	T	HcT	10.011	kOe
Bgap(Av)	0.778	T	PhiG	244.089	Lines	BgA/BgOC	0.976	
Bg1OC	0.952	T	PhiM1	232.783	Lines	Bg1/BgOC	1.188	
BmOC	0.890	T	Bm/BrT	0.854		f_Lkg	0.833	
HmOC	-1.496	kOe	Hm/HcT	-0.149		PC	5.988	
Btpk	1.373	T	Bsypk	1.252	T	Brypk	1.401	T
kT(form)	5.555	lbin/A	kE(form)	75.900	V/krpm			
kT(act)	5.619	lbin/A	kE(act)	76.763	V/krpm	eLLpk	268.669	V
MagTemp	75.000	DegC	eMax	1.046	V	Xrl	0.980	
BHmag	105.921	kJ/m3	Carter	1.019		XBtpk	1.000	
Am(hp)	1646.282	mm^2	Ag(hp)	1568.564	mm^2	CPhi	1.050	
pupa	0.817		Xrl	0.980		prl	0.100	
Rg(hp)	7.753E+05	At/Wb	1+PmO*Rg	1.204				
Btpk_oc	1.447	T	Btpk_ld	2.025	T	Btpk_ldS	2.024	T
Bfpk_oc	1.269	T	Bfpk_ld	1.404	T	Bfpk_ldS	1.404	T
kSatn_St	0.999		CalcSatn	Iterate		PFeMeth	Bpk_Ld_Fa	
kSatn_Dy	0.999		SlotMod	Yes		CalcCogg	No	

7 PM Dynamic design (time-stepping simulation):--------------------------------

OpMode	Motoring							
Torque	980.505	lbin	PowerSh	54.451	hp	Eff	92.520	%
LossCu	4.184	hp	LossFe_S	0.205	hp	LossWF_S	0.013	hp
LossTot	4.402	hp	TempRise	3.283	DegC	Jrms	16.754	A/mm^2
IWpk	180.516	A	IWav	111.149	A	IWrms	123.473	A
ILpk	180.516	A	ILav	111.149	A	ILrms	123.473	A
IQchpk	181.012	A	IQchav	39.491	A	IQchrms	75.014	A
IQcmpk	181.012	A	IQcmav	39.491	A	IQcmrms	75.014	A
IDchpk	180.154	A	IDchav	16.083	A	IDchrms	44.678	A
IDcmpk	180.154	A	IDcmav	16.083	A	IDcmrms	44.678	A
IDCLinkP	69.774	A	LossConv	1.031	hp	EffDCSh	90.927	%
Hystband	Constant		FreqChop	8.400	kHz			

8 Miscellaneous:---

WtCu	10.421	lb	WtFe	17.340	lb	WtMag	3.097	lb
WtTot	30.858	lb	RotJ	4.694E-03	lbfts2	LosFe/Wt	19.434	W/kg
IDCLinkW	70.465	A	sigma	13.082	psi	XFe	1.000	
Freq1	175.000	Hz	FreqChop	8.400	kHz			
TempCalc	DegCW		DegCW	1.000E-03	degC/W	HTranAct	22840.836	W/m2/C
Ambient	20.000	DegC	HTranEnd	0.000	W/m2/C			
HysBand	6.250	%	IntStep	0.250	eDeg			
WfO	2.000	hp	RPMO	20000.000	rpm	NWFT	1.880	
EMFCalc	BLV		Fringing	ON		XFringe	1.000	
CanStyle	None							

9 Core loss analysis:---

St.Steel NO10 0.1mm, 0.95 kstack.
Ro.Steel M19 29 gage

WtTeeth	7.592	lb	WtYoke	9.748	lb	WtTroot	1.592	lb
LossTthE	0.026	hp	LossTthH	0.120	hp	LossTth	0.146	hp
LTthE/Wt	4.636	W/kg	LTthH/Wt	21.503	W/kg	LTth/Wt	26.139	W/kg
LossYkE	5.354E-03	hp	LossYkH	0.053	hp	LossYk	0.059	hp
LYkE/Wt	0.906	W/kg	LYkH/Wt	9.038	W/kg	LYk/Wt	9.944	W/kg
LossE50	0.085	W/kg	LossH50	3.184	W/kg	LossFe50	3.269	W/kg
PFeMeth	Bpk_Ld_Fa		Btpk_ldS	2.024	T	Bfpk_ldS	1.404	T
FeF_E_OC	4.373E-03	hp	FeF_E_St	5.370E-03	hp	FeF_E_Dy	5.354E-03	hp
FeF_H_OC	0.039	hp	FeF_H_St	0.054	hp	FeF_H_Dy	0.053	hp
FeT_E_OC	0.013	hp	FeT_E_St	0.026	hp	FeT_E_Dy	0.026	hp
FeT_H_OC	0.055	hp	FeT_H_St	0.120	hp	FeT_H_Dy	0.120	hp
Fe_OC	0.112	hp	Fe_Ld_St	0.205	hp	Fe_Ld_Dy	0.205	hp

End of Design sheet--

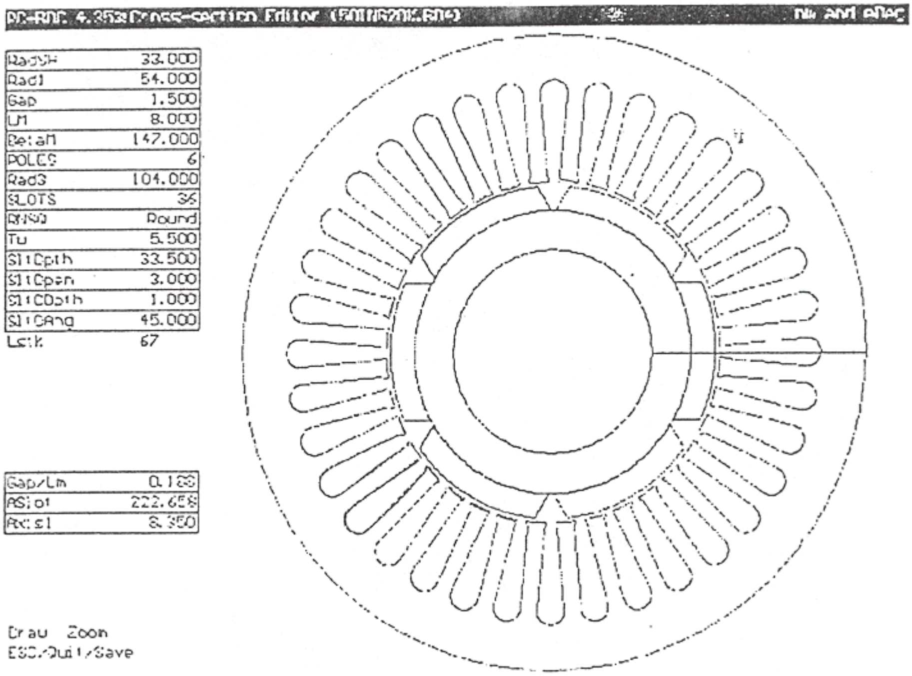

FIG. 6 CROSS SECTION OF 50/20 MOTOR

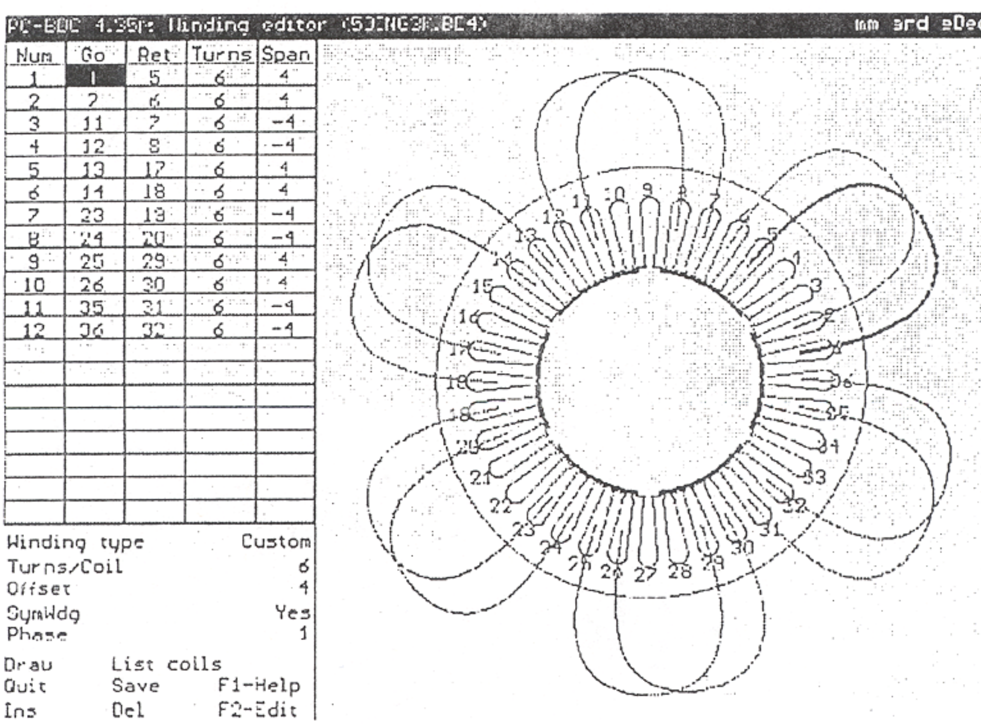

FIG. 7 PHASE WINDING OF 50/20 MOTOR

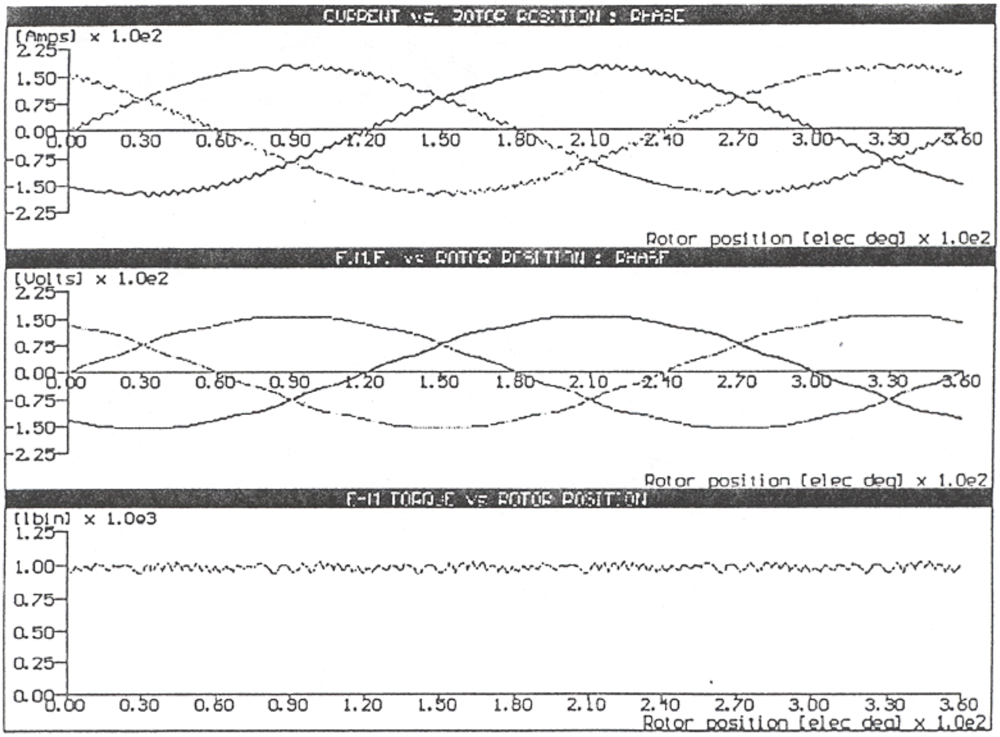

FIG. 8 PHASE CURRENT, BACK EMF & TORQUE VS ANGLE,

50/20 MOTOR AT 3500 RPM

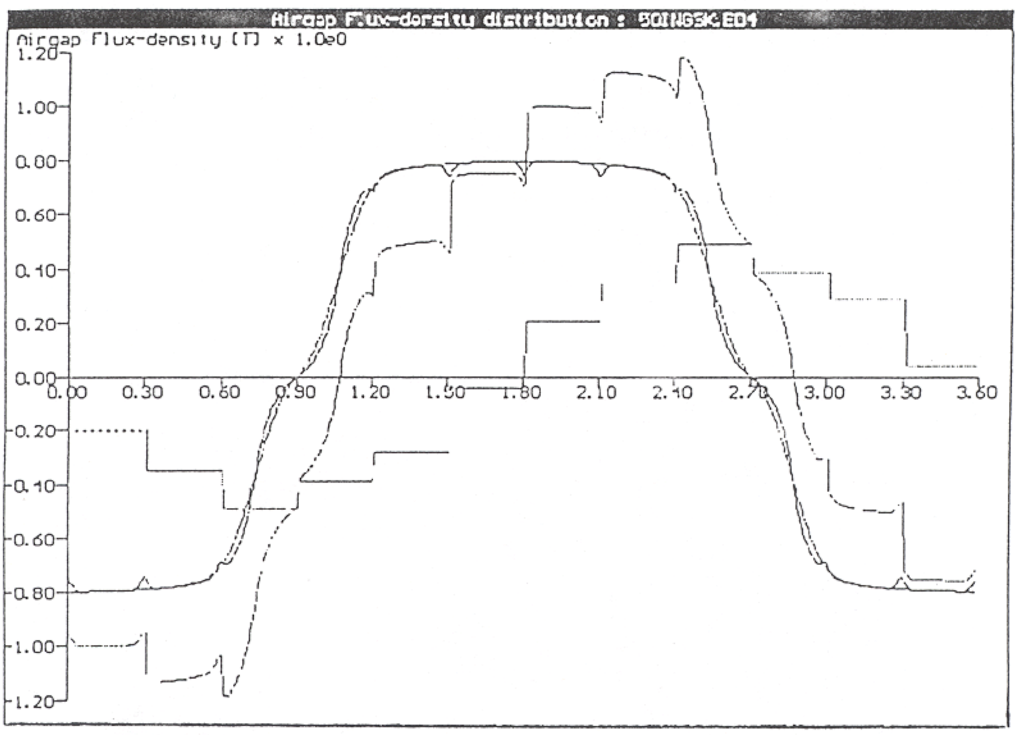

FIG. 9 AIR GAP FLUX OF 50/20 MOTOR AT 3500 RPM

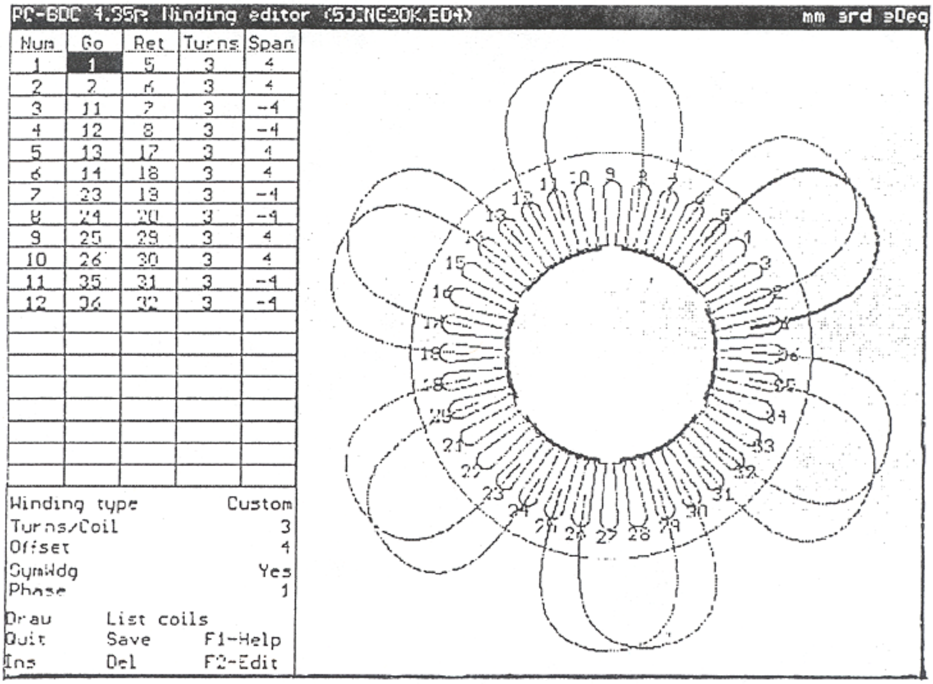

FIG. 10 PHASE WINDING OF 50/20 MOTOR

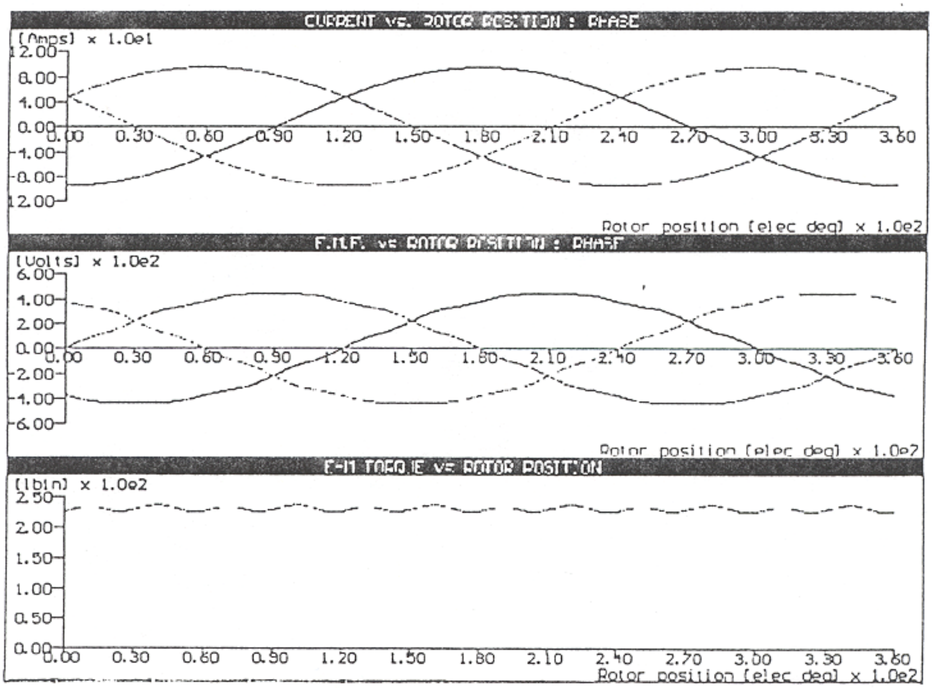

FIG. 11 PHASE CURRENT, BACK EMF & TORQUE VS ANGLE, 50/20 MOTOR

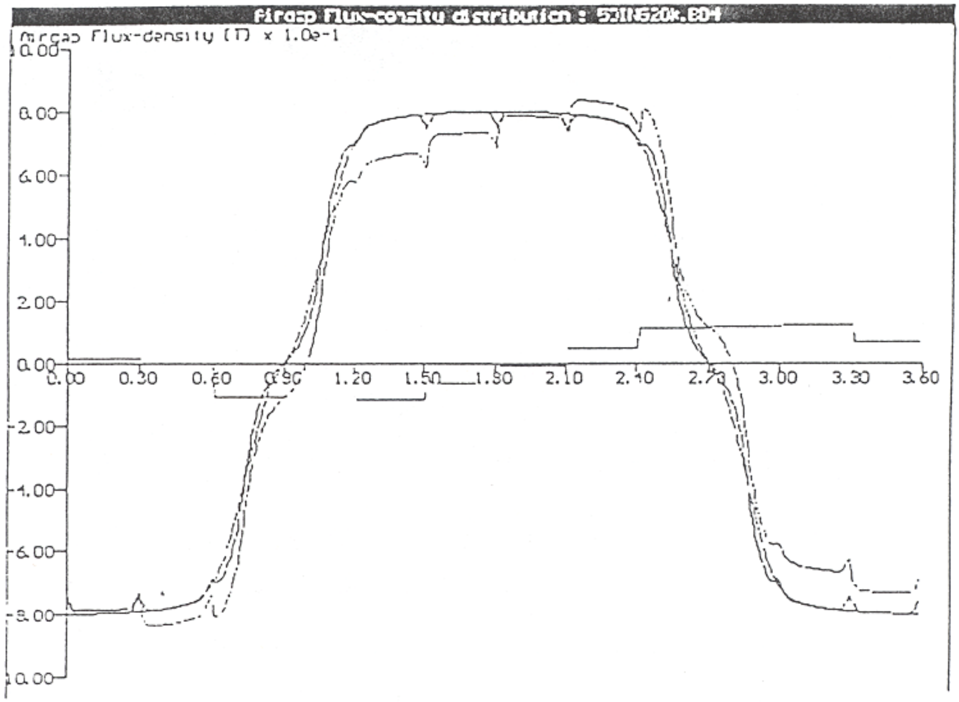

FIG. 12 PHASE CURRENT, BACK EMF & TORQUE ANGLE
VS ANGLE, 50/20 MOTOR AT 20,000 RPM

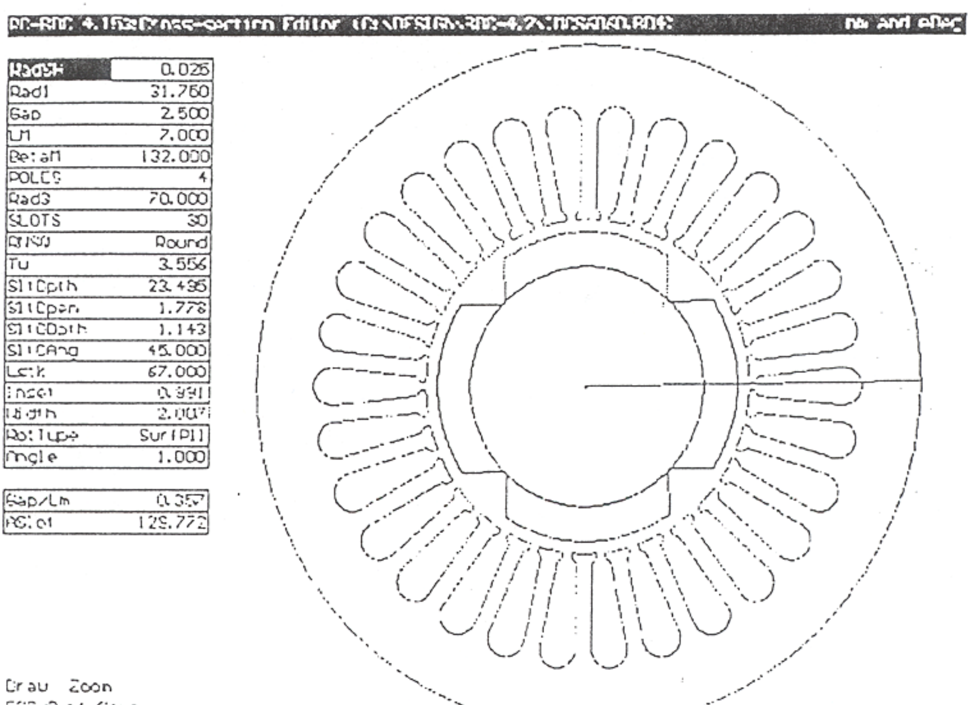

FIG. 13 CROSS SECTION OF 60/60 MOTOR

TABLE 3A

PC-BDC 4.35Ã: 25th Mar 1996 21:52 50ING20K.BD4
JR Hendershot Magna Physics Tridelta
PC-BDC Main Title
PC-BDC Sub-title

1 Dimensions:--

RadSH	33.000 mm	Rad1	54.000 mm	Gap	1.500 mm
LM	8.000 mm	BetaM	147.000 eDeg	POLES	6
Rad2	89.000 mm	Rad3	104.000 mm	SLOTS	36
Tw	5.500 mm	SltDpth	33.500 mm	SltOpen	3.000 mm
SltODpth	1.000 mm	SltOAng	45.000 mDeg	RNSQ	Round
SYoke	15.000 mm	RYoke	6.837 mm	Skew	0.670
Lstk	67.000 mm	Stf	0.970	MOH	4.000 mm

2 Magnet Data:---

Magnet	R26H	RotType	SurfPll	PmO	0.264 uWb/A-t
Br	1.060 T	HcJ	10.179 kOe	MuRec	1.020
CBr	-0.030 %/DegC	CHcJ	-0.030 %/DegC	DMag	8400.000 kg/m3

3 Control Data:--

Drive	Sine	Vs	640.000 V	RPM	20000.000 rpm
ISP	95.000 A	gamma	30.000 deg	Sw_Ctl	ISP_HB
Vq	3.000 V	Rq	0.000 Ohms	Vd	1.200 V
ISP_Act	95.000 A	HBA_Act	16.000 %	ISLA_Act	128.000

4 Winding Data:--

WdgType	Custom	Connex	3-Ph Wye		
Offset	4	Coils/P	2.000	NSH	36
Tph	36.000	PPATHS	1	SPP	2.000
Layers	2.000	CSidesPh	24	Z	216.000
MLT	337.439 mm	LgthOEnd	137.571 mm	Ext	8.000 mm
EndFill	0.500	LaxPack	101.370 mm	TFRho	1.217
SFill	0.199	Gauge	24.000	WireSpec	AWGTable
SFillHBL	0.344	WireDia	0.511 mm	Liner	0.254 mm
SlotArea	222.658 mm^2	CondArea	7.370 mm^2	ASlotLL	203.826 mm^2
WdgTemp	75.000 DegC	Rph	0.034 Ohm/Ph	Rterm	0.068 Ohms
Lph	0.139 mH/Ph	Mph	-0.059 mH/Ph	Lterm	0.396 mH
Lg	0.075 mH/Ph	LSlot	0.044 mH/Ph	Lendt	0.020 mH/Ph
Mg	-0.038 mH/Ph	MSlot	-0.022 mH/Ph	fz	1.142
PCSlot	2.415	XLph	1.000	XET	1.000
Ax1	38.350 mDeg				
iA_Ang	-75.994 A	iB_Ang	17.941 A	iC_Ang	58.053 A
ks1	0.995	kp1	0.837	kd1	1.000
kw1	0.832	XmO	4.179 Ohm/Ph	Xd	1.080 Ohm/Ph
Nse	38.147	Xsigma	0.399	Xq	1.077 Ohm/Ph
Cd	0.163	Cq	0.162	k1	0.000
k1ad	0.000	k1aq	0.000	kAlphad	0.000
NumPoly	1				

5 Magnetic Circuit Design:---

BrT	1.043 T	BgOC	0.797 T	HcT	10.011 kOe
Bgap(Av)	0.778 T	PhiG	244.089 Lines	BgA/BgOC	0.976
Bg1OC	0.952 T	PhiM1	232.783 Lines	Bg1/BgOC	1.188
BmOC	0.890 T	Bm/BrT	0.854	f_Lkg	0.833
HmOC	-1.496 kOe	Hm/HcT	-0.149	PC	5.988
Btpk	1.373 T	Bsypk	1.252 T	Brypk	1.401 T
kT(form)	2.778 lbin/A	kE(form)	37.950 V/krpm		
kT(act)	2.433 lbin/A	kE(act)	33.239 V/krpm	eLLpk	664.783 V
MagTemp	75.000 DegC	eMax	5.978 V	Xrl	0.980
BHmag	105.921 kJ/m3	Carter	1.019	XBtpk	1.000
Am(hp)	1646.282 mm^2	Ag(hp)	1568.564 mm^2	CPhi	1.050
pupa	0.817	Xrl	0.980	prl	0.100
Rg(hp)	7.753E+05 At/Wb	1+PmO*Rg	1.204		
Btpk_oc	1.447 T	Btpk_ld	1.443 T	Btpk_ldS	1.443 T
Bfpk_oc	1.269 T	Bfpk_ld	1.208 T	Bfpk_ldS	1.208 T
kSatn_St	1.000	CalcSatn	Iterate	PFeMeth	Bpk_Ld_Fa
kSatn_Dy	1.000	SlotMod	Yes	CalcCogg	No

TABLE 3B

7 PM Dynamic design (time-stepping simulation):-------------------------------

OpMode	Motoring				
Torque	173.036 lbin	PowerSh	54.910 hp	Eff	93.992 %
LossCu	0.448 hp	LossFe_S	1.062 hp	LossWF_S	2.000 hp
LossTot	3.510 hp	TempRise	2.617 DegC	Jrms	7.750 A/mm^2
IWpk	79.337 A	IWav	50.661 A	IWrms	57.112 A
ILpk	79.337 A	ILav	50.661 A	ILrms	57.112 A
IQchpk	79.603 A	IQchav	23.939 A	IQchrms	39.861 A
IQcmpk	79.603 A	IQcmav	23.939 A	IQcmrms	39.861 A
IDchpk	59.219 A	IDchav	1.393 A	IDchrms	6.492 A
IDcmpk	59.219 A	IDcmav	1.393 A	IDcmrms	6.492 A
IDClinkP	68.749 A	LossConv	0.585 hp	EffDCSh	93.061 %
Hystband	Constant	FreqChop	14.000 kHz		

8 Miscellaneous:---

WtCu	5.211 lb	WtFe	17.340 lb	WtMag	3.097 lb
WtTot	25.647 lb	RotJ	4.694E-03 lbfts2	LosFe/Wt	107.360 W/kg
IDCLinkW	68.874 A	sigma	2.392 psi	XFe	1.000
Freq1	1000.000 Hz	FreqChop	14.000 kHz		
TempCalc	DegCW	DegCW	1.000E-03 degC/W	HTranAct	22840.836 W/m2/C
Ambient	20.000 DegC	HTranEnd	0.000 W/m2/C		
HysBand	6.250 %	IntStep	0.250 eDeg		
Wf0	2.000 hp	RPM0	20000.000 rpm	NWFT	1.880
EMFCalc	BLV	Fringing	ON	XFringe	1.000
CanStyle	None				

9 Core loss analysis:--

St.Steel NO10 0.1mm, 0.95 kstack.
Ro.Steel M19 29 gage

WtTeeth	7.592 lb	WtYoke	9.748 lb	WtTroot	1.592 lb
LossTthE	0.428 hp	LossTthH	0.308 hp	LossTth	0.801 hp
LTthE/Wt	81.902 W/kg	LTthH/Wt	61.405 W/kg	LTth/Wt	143.308 W/kg
LossYkE	0.130 hp	LossYkH	0.196 hp	LossYk	0.332 hp
LYkE/Wt	22.192 W/kg	LYkH/Wt	33.769 W/kg	LYk/Wt	55.961 W/kg
LossE50	0.085 W/kg	LossH50	3.184 W/kg	LossFe50	3.269 W/kg
PFeMeth	Bpk_Ld_Fa	Btpk_ldS	1.443 T	Bfpk_ldS	1.208 T
FeF_E_OC	0.143 hp	FeF_E_St	0.132 hp	FeF_E_Dy	0.130 hp
FeF_H_OC	0.225 hp	FeF_H_St	0.200 hp	FeF_H_Dy	0.196 hp
FeT_E_OC	0.435 hp	FeT_E_St	0.458 hp	FeT_E_Dy	0.428 hp
FeT_H_OC	0.316 hp	FeT_H_St	0.343 hp	FeT_H_Dy	0.308 hp
Fe_OC	1.119 hp	Fe_Ld_St	1.132 hp	Fe_Ld_Dy	1.062 hp

End of Design sheet---

5. 60 HP, 60 KRPM BRUSHLESS MOTOR

The other example of a high speed motor application involves vapor cycle compressors for heat pumps for large buildings such as office buildings, apartment complexes and shopping malls. The physical size of the unit can be substantiality reduced (by a factor of 4 to 6 even more) if centrifugal impellers are driven at very high speeds. These can be singles, double or three stage centrifugal compressors. The details and merits of this concept are beyond the scope of this paper. However there is a serious and wide spread interest in the use of high speed motors for these compressors.

A 60/60 PM brushless motor design is summarized for one of these applications. This motor converts 60 KW at 60,000 RPM. The rotor is a 4 pole design as shown on Figure 13 which depicks the rotor and stator cross section. The pole arcs are properly selected to minimize cogging. The stator laminations are punched from very thin (0.005") very low core loss magnetic iron coated with a C-5 core plate for inter-laminar insulation from eddy currents.

The samarium cobalt magnets are secured to the solid shaft (alloy steel) with a pre-stressed carbon composite casement. The stator design is based upon (30) slots and a special winding with ten coils per phase. The performance was achieved with (2) turns per coil of #24 AWG wire with (48) strands in parallel to minimize the skin affect and eddy currents. The windings establish (4) poles with the (10) coils using (2) coils for two poles and (3) coils for the other (2) poles for a total of (10) coils.

Figures 14 and 15 show the winding pattern of one phase and the total windings respectfully. There are (4) conductor per slot for a total (Z) of (120) conductors. Figure 13 shows the winding pattern of one phase with the other two phases displaced (5) slots apart. (This very unique winding for 4 pole high speed fractional slot motors was furnished to this author by a good friend and skilled magnetician by the name of Homar Lazar of Santa Barbara, CA.)

Figure 16 plots the current, back EMF and torque vs rotor angle. The data is simulated at 60,000 RPM driven by a trapezoid 6 step inverter. The simulated torque ripple cannot be measured at these speeds so the simulation of this ripple is very important to study.

The compressor application requires increasing output power with speed due to the behavior of the centrifugal impellers rather than constant HP required from the machine tool spindle. This means that the magnets do not need to be as thick which makes retainment more manageable at these high speeds. Figure 16 shows the open current air gap flux over one pole. The full load current effects are also shown with the super imposed flux distortion plot on Figure 17. Figure 18 shows a plot of output efficiency vs RPM. The constantcy of the 94% or so over a 10 KRPM to 60 KRPM is very important for these heat pump compressors. The PM motor achieves the highest efficiency over the operating speed range of any electric motor known at the present time. Finally table 4 provides all of the detailed design output data as well as the input parameters. The results were developed using the PC-BDC simulation software from the University of Glasgow.

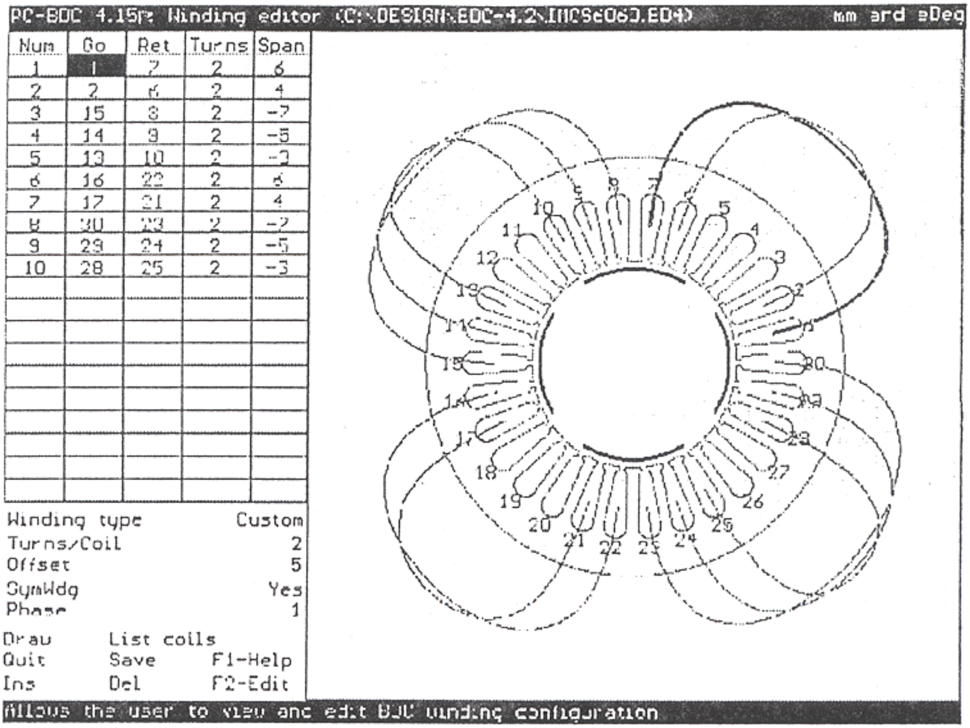

FIG. 14 PHASE WINDING 60/60 MOTOR

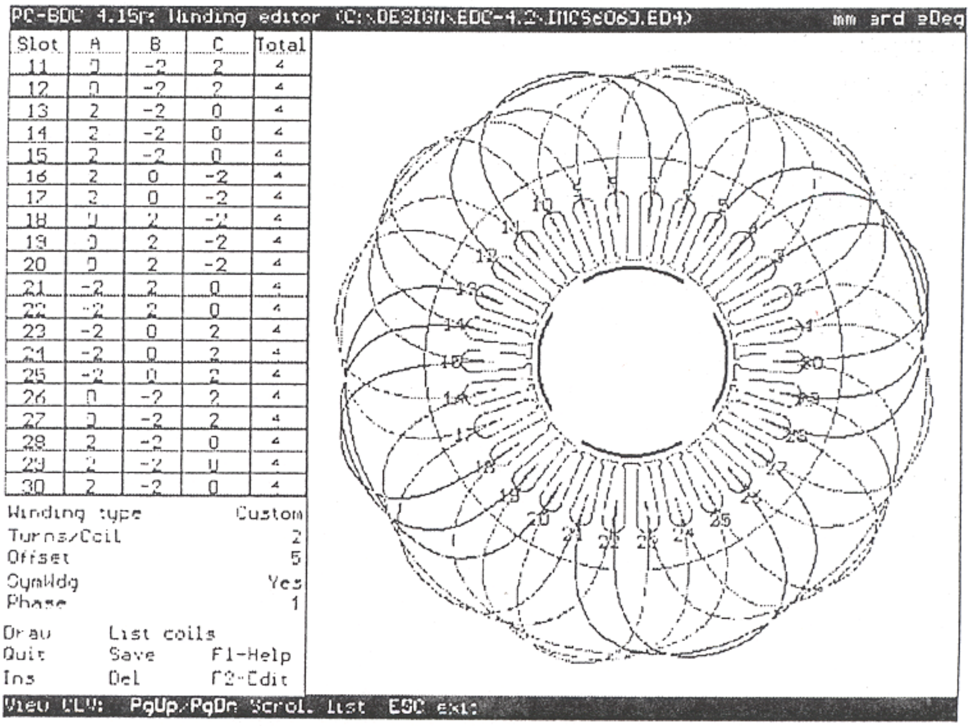

FIG. 15 ALL PHASES OF 60/60 MOTOR

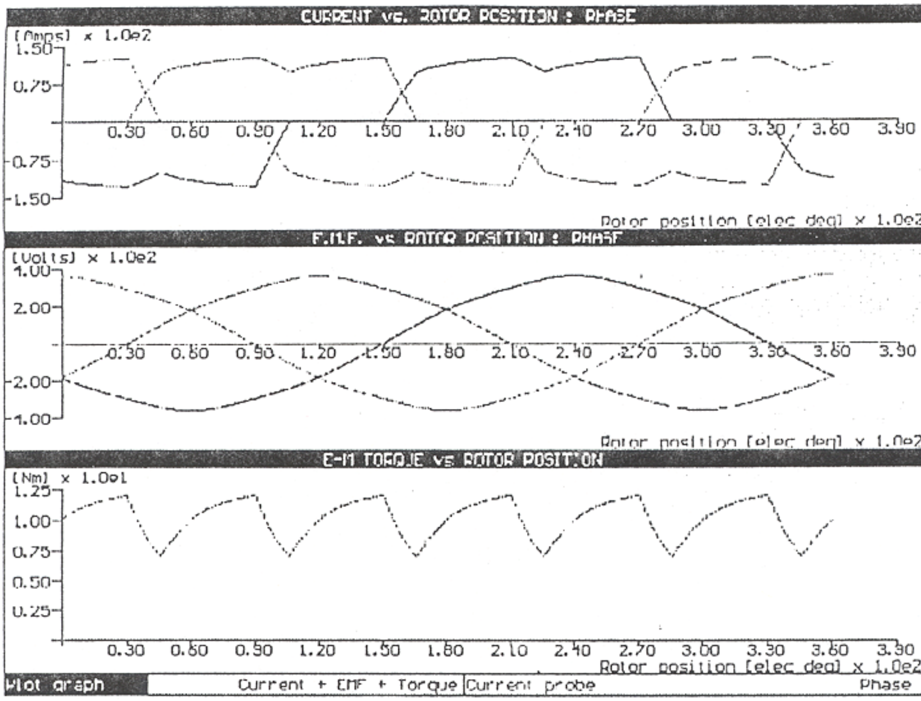

FIG. 16 PHASE CURRENT, BACK EMF & TORQUE OF 60/60 MOTOR AT 60 KRPM

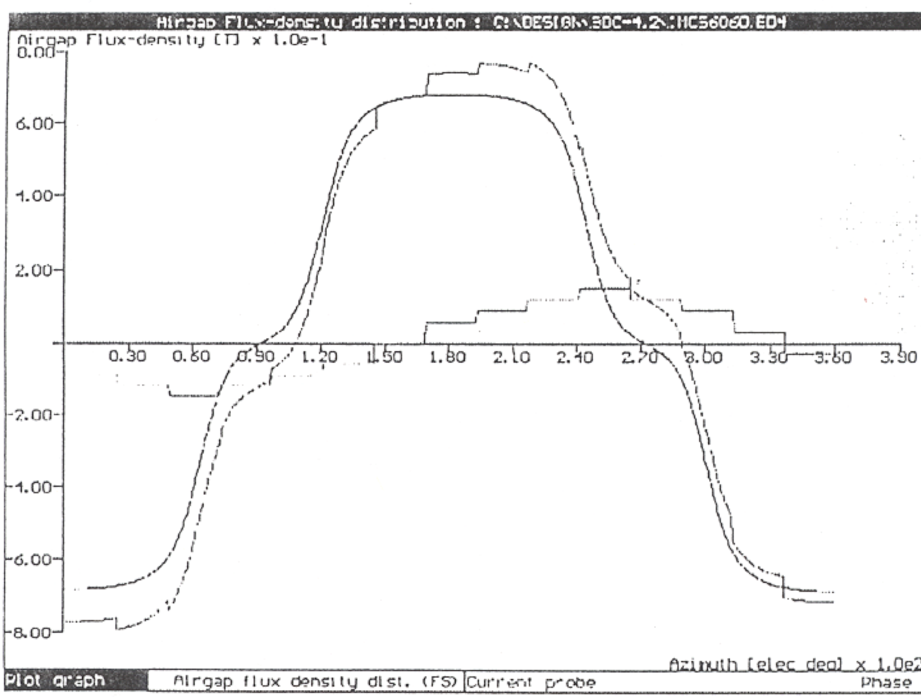

FIG. 17 AIR GAP FLUX OF 60/60 MOTOR AT 60,000 RPM

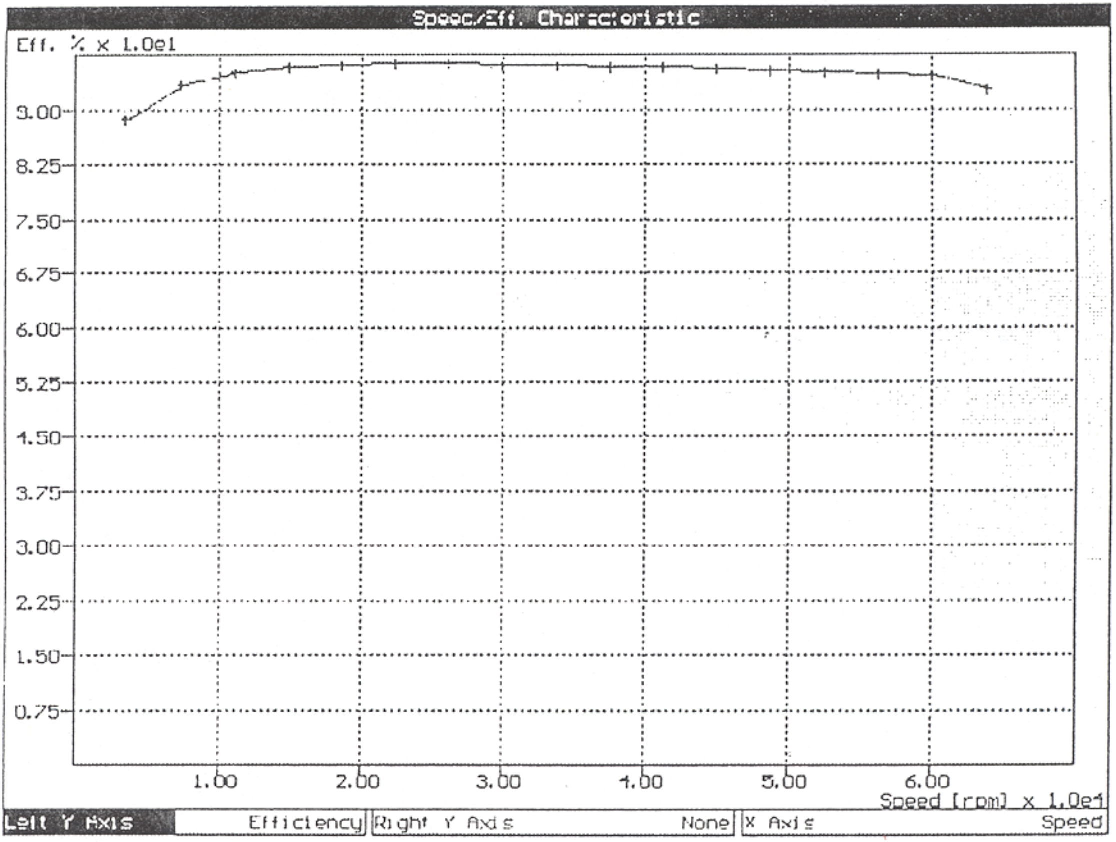

FIG. 18 EFFICIENCY VS SPEED FOR 60/60 MOTOR

TABLE 4A

PC-BDC 4.15Ã: 19th Mar 1996 17:21 C:\DESIGN\BDC-4.2\IMCS6060.BD4
Magna Physics (JRH) (TJEM Visit 4-29-95)
PC-BDC Main Title
PC-BDC Sub-title

1 Dimensions:--

RadSH	0.025	mm	Rad1	31.750	mm	Gap	2.500	mm
LM	8.000	mm	BetaM	124.000	eDeg	POLES	4	
Rad2	57.745	mm	Rad3	70.000	mm	SLOTS	30	
Tw	3.556	mm	SltDpth	23.495	mm	SltOpen	1.778	mm
SltODpth	1.143	mm	SltOAng	45.000	mDeg	RNSQ	Round	
SYoke	12.255	mm	RYoke	23.725	mm	Skew	0.670	
Lstk	67.000	mm	Stf	0.970		MOH	4.000	mm

2 Magnet Data:--

Magnet	R26H		RotType	SurfPll		Pm0	0.189	uWb/A-t
Br	1.060	T	HcJ	8.100E+05	A/m	Murec	1.020	
CBr	-0.030	%/Deg.C	CHcj	-0.030	%/Deg.C	DMag	8400.000	kg/m3

3 Control Data:--

Wave	Square		Vs	640.000	V	RPM	60000.000	rpm
ISP	130.000	A	THO	30.000	eDeg	Sw_Ctl	C60_Q1	
Vq	3.000	V	Rq	0.000	Ohms	Vd	1.200	V

4 Winding Data:--

WdgType	Custom		Connex	3-Ph Wye				
Offset	5		Coils/P	2.500		NSH	48	
Tph	20.000		PPATHS	1		SPP	2.500	
Layers	2.000		CSidesPh	20		Z	120.000	
MLT	429.219	mm	LgthOEnd	200.217	mm	Ext	7.620	mm
EndFill	0.500		LaxPack	129.971	mm	TFRho	1.020	
SFill	0.303		Gauge	24.000		WireSpec	AWGTable	
SFillHBL	0.535		WireDia	0.511	mm	Liner	0.254	mm
SlotArea	129.772	mm^2	CondArea	9.826	mm^2	ASlotLL	116.530	mm^2
WdgTemp	25.000	DegC	Rph	0.015	Ohm/Ph	Rterm	0.030	Ohms
Lph	0.059	mH/Ph	Mph	-0.023	mH/Ph	Lterm	0.072	mH
Lg	0.029	mH/Ph	LSlot	0.016	mH/Ph	Lendt	0.013	mH/Ph
Mg	-0.014	mH/Ph	MSlot	-0.008	mH/Ph	fz	1.157	
PCSlot	2.426		XLph	1.000		XET	1.600	
Ax1	52.020	mDeg						

5 Magnetic Circuit Design:--

BrT	1.019	T	BgOC	0.682	T	HcT	778.410	kA/m
Bgap(Av)	0.662	T	PhiG	1.643	mWb	BgA/BgOC	0.971	
Bg1OC	0.736	T	PhiM1	1.688	mWb	Bg1/BgOC	1.079	
BmOC	0.805	T	Bm/BrT	0.790		f_Lkg	0.833	
HmOC	-166.499	kA/m	Hm/HcT	-0.214		PC	3.862	
Btpk	1.318	T	Bsypk	0.994	T	Brypk	0.498	T
kT(form)	1.075	lbin/A	kE(form)	12.722	V/krpm	RPMnlKEf	49836.198	rpm
kT(act)	0.711	lbin/A	kE(act)	8.415	V/krpm	RPMnlKEa	75343.125	rpm
eLLpk	504.890	V	eMax	9.193	V	MagTemp	150.000	DegC
IBk	-186.227	A	Bk	1.000	T	Hk	-14.558	kA/m
ILR	20931.416	A	BmLR	-24.690	T	HmLR	-20057.343	kA/m
IC180	37600.288	A	BmC180	-44.968	T	HmC180	-35877.794	kA/m
BHmag	134.073	kJ/m3	Carter	1.008		XBtpk	1.000	
Am(hp)	1180.170	mm^2	Ag(hp)	1196.266	mm^2	CPhi	0.987	
pupa	0.689		Xrl	0.980				
Rg(hp)	1.677E+06	At/Wb	1+Pm0*Rg	1.317				

TABLE 4B

7 PM Dynamic design (time-stepping simulation):--------------------------------

OpMode	Motoring							
Torque	10.112	Nm	PowerSh	63.535	kW	Eff	94.657	%
LossCu	0.401	kW	LossFe_S	3.186	kW	LossWF_S	0.000	kW
LossTot	3.587	kW	TempRise	35.866	DegC	Jrms	9.560	A/mm^2
IWpk	128.354	A	IWav	78.153	A	IWrms	93.938	A
ILpk	128.354	A	ILav	78.153	A	ILrms	93.938	A
IQchpk	128.354	A	IQchav	35.988	A	IQchrms	64.298	A
IQcmpk	128.788	A	IQcmav	35.988	A	IQcmrms	64.298	A
IDchpk	128.563	A	IDchav	2.733	A	IDchrms	15.241	A
IDcmpk	0.000	A	IDcmav	2.733	A	IDcmrms	15.241	A
IDClinkP	105.921	A	LossConv	0.667	kW	EffDCSh	93.725	%

8 Miscellaneous:--

WtCu	2.227	kg	WtFe	3.770	kg	WtMag	0.707	kg
WtTot	6.703	kg	RotJ	7.261E-04	kg-m2	LosFe/Wt	845.075	W/kg
IDCLinkW	104.743	A	sigma	3.453	psi	XFe	1.000	
Freq1	2000.000	Hz	FreqChop	0.000	kHz			
TempCalc	DegCW		DegCW	1.000E-02	degC/W	HTranAct	3393.496	W/m2/C
Ambient	20.000	DegC	HTranEnd	0.000	W/m2/C			
HysBand	3.125	%	IntStep	0.031	eDeg			
Wf0	0.000	kW	RPM0	40000.000	rpm	NWFT	2.000	
EMFCalc	BLV		Fringing	ON		XFringe	1.000	

9 Core loss analysis:--

St.Steel M19 29 gage
Ro.Steel M19 29 gage

WtTeeth	1.379	kg	WtYoke	2.391	kg	WtTroot	0.318	kg
LossTthE	2.288	kW	LossTthH	0.104	kW	LossTth	2.391	kW
LTthE/Wt	1348.416	W/kg	LTthH/Wt	61.131	W/kg	LTth/Wt	1409.547	W/kg
LossYkE	0.706	kW	LossYkH	0.089	kW	LossYk	0.794	kW
LYkE/Wt	295.151	W/kg	LYkH/Wt	37.068	W/kg	LYk/Wt	332.219	W/kg
LossE50	0.357	kW	LossH50	1.976	kW	LossFe50	2.333	kW

End of Design sheet---

6. SUMMARY

The PM brushless motor can be the premier prime mover for several emerging applications requiring high speed and high power outputs. The strength and robustness of modern rare earth magnets allow these motors to achieve constant HP over a very wide speed range, not thought to be possible. At the other extreme of applications, constant high efficiency over a very wide speed range with somewhat constant torque is achievable with these machines. They are quite expensive compared to other motors when considered as a system component. However their cost increase buys performance gains which can actually reduce total system cost by a substantial amount.

7. REFERENCES

(1) JR Hendershot Jr, TJE miller: "Design of Brushless Permanent-Magnet Motors", ISBN 1-881855-03-1, Magna Physics Publishers & Oxford University Press, 1994

(2) Duane C. Hanselman, "Brushless Permanent-Magnet Motor Design", ISBN 0-07-026025-7, McGraw-Hill, 1994

(3) Alexander H. Slocum, "Presision machine Design", Chapter 8 & 9, ISBN 0-13-690918-3, Prentice Hall, 1992